

# Plethora of Coexisting Topological Band Degeneracies in Nonsymmorphic Molecular Crystal OsOF<sub>5</sub>

Hyungjun Lee<sup>1,2,\*</sup> and Oleg V. Yazyev<sup>1,2,†</sup>

<sup>1</sup>*Institute of Physics, École Polytechnique Fédérale de Lausanne (EPFL), CH-1015 Lausanne, Switzerland*

<sup>2</sup>*National Centre for Computational Design and Discovery of Novel Materials MARVEL, École Polytechnique Fédérale de Lausanne (EPFL), CH-1015 Lausanne, Switzerland*

(Dated: March 17, 2022)

In band theory of solids, degeneracies manifest themselves as point, line, and surface objects. The topological nature of band degeneracies has recently been appreciated since the recognition of gapless topological quantum phases of matter. Based on first-principles calculations, we report the topological semimetal phase in osmium oxyhalide OsOF<sub>5</sub> that exhibits zero-dimensional Weyl points, one-dimensional nodal lines, and two-dimensional nodal surfaces. The semimetal phase is ensured by the electron filling constraint while band degeneracies of various dimensionalities are protected by the nonsymmorphic crystalline symmetries. Focusing on two nodal loops crossing the Fermi level, we demonstrate their topological protection by  $\pi$  Berry phase and describe the drumhead surface states topologically connected by nontrivial  $\mathbb{Z}_2$  index. Our prediction highlights OsOF<sub>5</sub> as a unique topological material in which a rich variety of topological degeneracies exists in a narrow energy range close to the Fermi level owing to the molecular crystal structure of this material.

Symmetry is one of the fundamental guiding principles of nature [1]. In physics, various kinds of discrete or continuous symmetries play a conscious role as the guides to physical laws and phenomena, and serve as one of the organizing principles in their classification [2]. Not only does its notion facilitate the more concise and elegant description of physical systems and phenomena, but also its invariance and violation give rise to the emergence of a host of physical phenomena [3, 4]. Symmetry constrains the allowable dynamics in physical systems [5] and implies the conservation laws [6]. Symmetry breaking had been serving as an organizing principle in the classification of possible phases of matter and transitions between them [7] before the recognition of topological order [8].

Symmetry is also at the heart of the degeneracy in electronic bands in crystalline solids. Given a symmetry group under which the Hamiltonian of the system of interest is invariant, we can use the symmetry to determine the existence and order of degenerate levels [9]. This study of degeneracies in crystals traces back to the early days of the band theory of solids: Bouckaert *et al.* [10] tackled this problem with an emphasis on the degeneracy necessitated by symmetry, the so-called essential degeneracy, and Herring addressed another type of degeneracy occurring in crystals, namely the accidental degeneracy [11], in a sense that degeneracy is not a direct consequence of symmetry.

Recently, the subject of degeneracy in the energy bands of crystals has been reignited by the theoretical predictions of topological semimetal phases of matter [12, 13], in which the valence and conduction bands touch at discrete points or continuous lines, forming low-dimensional Fermi surfaces. Similar to their insulating counterparts, topological (semi)metallic phases have topologically protected boundary modes, such as the surface

Fermi arcs [12], and display exotic transport properties such as the chiral anomaly [14].

Both gapped and gapless topological phases rely on the symmetry of the system. For instance, the nontrivial topology in topological insulators (TIs) is related to their time-reversal symmetry (TRS)  $\mathcal{T}$  and that of the topological crystalline insulators pertains to the crystalline symmetry. In the case of gapless topological phases, Weyl semimetals (WSMs) require the translational symmetry and Dirac semimetals (DSMs) need additional crystalline symmetries such as rotational symmetry to stabilize their band touching points [15]. In particular, crystalline symmetries are diverse and one can expect a host of nontrivial topology which originate from them [16, 17]. Among the symmetry-protected topological phases, topological nodal-line semimetals, one of the possible topological semimetal phases [15, 18], attract much interest as a fertile ground for exploring the interplay between topology and symmetry [19], as well as the intermediate phase in the transitions to other topological phases such as TIs [20], WSMs [21, 22] and DSMs [23, 24].

In this Letter, we report the discovery of a novel topological semimetal phase in OsOF<sub>5</sub> enforced by its electron filling under the combination of time-reversal and nonsymmorphic crystalline symmetries. The material exhibits a rich variety of coexisting topological band degeneracies of various dimensionalities close to the Fermi energy ( $E_F$ ), namely the zero-dimensional (0D) Weyl points, one-dimensional (1D) nodal lines, and two-dimensional (2D) nodal surfaces. Focusing on two nodal loops crossing  $E_F$ , we demonstrate their nontrivial topology of  $\pi$  Berry phase and describe the drumhead surface states topologically connected by nontrivial  $\mathbb{Z}_2$  index. Our work adds to the family of topological materials a new member that is unique in a sense that the multitude



a gapless phase at filling  $\nu = 8n + 4$ .

The second remarkable feature is the connected eight-band manifold. A group of bands is called “connected” if one can travel continuously through all its branches owing to the touching points between them [33]. To clearly demonstrate it, we plot the band dispersions along the U-X- $\Gamma$  and the U-X lines [Figs. 2(b) and (c), respectively]. The presence of the connected eight-band manifold and its robustness can be explained by symmetry arguments. All  $k$  points along the U-X line are invariant under three nonsymmorphic symmetry operations  $-\tilde{M}_x$ ,  $\tilde{M}_y$ , and  $\tilde{C}_{2z}$ . Thus, the energy eigenstates can be labeled simultaneously with the eigenvalues of these nonsymmorphic symmetry operators. On the other hand, for  $k$  points along the  $\Gamma$ -X line, only  $\tilde{M}_y$  belongs to the little co-group. On the glide-invariant planes, the eigenvalues of  $\tilde{M}_x$  and  $\tilde{M}_y$ , denoted as  $\tilde{m}_x$  and  $\tilde{m}_y$ , can be written as  $\tilde{m}_x(\mathbf{k}) = \pm ie^{-i(k_y b + k_z c)/2}$  and  $\tilde{m}_y(\mathbf{k}) = \pm ie^{-ik_x a/2}$ . It follows that for the time-reversal-invariant momentum (TRIM) points  $\Gamma$  and X on the  $\Gamma$ -X line, the twofold-degenerate Kramers partners have the opposite eigenvalues  $\tilde{m}_y = \pm i$  at  $\Gamma$ , but at X they should have the same eigenvalue  $\tilde{m}_y = +1$  or  $\tilde{m}_y = -1$  owing to the Kramers degeneracies between the complex-conjugate representations at the TRIM points. This results in partner switching between the two TRIM points due to the continuity of glide eigenvalues, and thus leads to an unavoidable band crossing between  $\Gamma$  and X, forming the connected “four-band” group with the hourglass-shaped dispersion, the typical building-block of the band structure of nonsymmorphic crystals with SOC and TRS [34–36].

In order to confirm the fact that instead of four bands, eight bands should be tangled together in SG  $Pna2_1$ , one has to check additionally the evolution of glide eigenvalues along the X-U line where  $\tilde{M}_x$  and  $\tilde{M}_y$  are the elements of the little group. While  $\tilde{m}_y$  is constant with the value of  $+1$  or  $-1$ ,  $\tilde{m}_x$  along the X-U line shows the same hourglass-type evolution. Importantly, due to the continuity of the glide eigenvalues, the partners of the states should be exchanged again along this line, resulting in a band dispersion that represents two overlapping hourglasses [35]. The reasoning above is also confirmed by the evolution of glide eigenvalues shown in Figs. 2(b) and (c), which are directly calculated from *ab initio* Bloch states. It is this type of eight-band connectivity that explains why  $\nu = 8n + 4$  implies a semimetal phase [31] for SG  $Pna2_1$ . Bearing in mind this along with the fact that the level repulsion can be avoided between the states belonging to different irreducible representations, we can confirm that there are irremovable band touching points along these high-symmetry lines arising due to the nonsymmorphic symmetries.

We can expect that these band degeneracies are part of symmetry-protected nodal-line structures on the glide-invariant planes [36] including the  $\Gamma$ -X or X-U line. In order to verify this suggestion and identify the complete

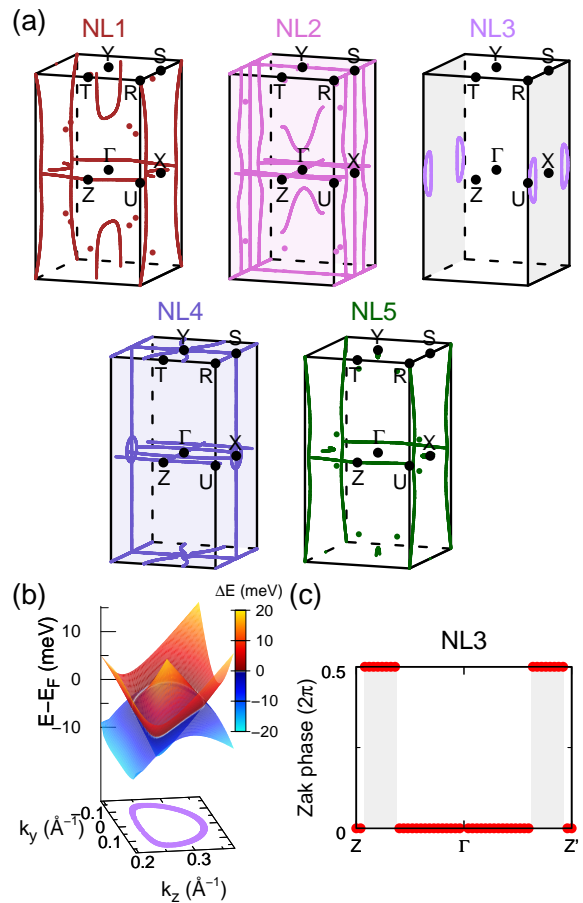


FIG. 3. (a) Band degeneracies of different dimensionalities in OsOF<sub>5</sub> formed by band crossings between bands  $(N - 2)$  and  $(N - 1)$  (NL1),  $(N - 1)$  and  $N$  (NL2),  $N$  and  $(N + 1)$  (NL3),  $(N + 1)$  and  $(N + 2)$  (NL4), and, finally, bands  $(N + 2)$  and  $(N + 3)$  (NL5). Here,  $N$  is the number of valence electrons in the unit cell. In NL2 (NL4), the nodal surfaces at  $k_z = \pm\pi/c$  are highlighted by shaded planes. (b) Band dispersion around the nodal loop (NL3). Bands are encoded by the color corresponding to the energy difference between the lowest conduction and highest valence bands. The contour of the nodal loop is plotted underneath. (c) Evolution of Zak phase for the nodal loop (NL3) along the high-symmetry line from Z  $(0, 0, \pi/c)$  to Z'  $(0, 0, -\pi/c)$ .

structure of degeneracies, we performed the direct search of all possible band degeneracies. We found band degeneracies of different dimensionalities such as 0D Weyl points, 1D nodal lines, and finally 2D nodal surfaces, as summarized in Fig. 3(a). Their detailed descriptions are in order. First, there are two nodal loops on the BZ boundary with  $k_x = \pm\pi/a$ , which result from the twofold degeneracy between bands  $N$  and  $(N + 1)$  (NL3), where  $N$  is the number of valence electrons in the unit cell. These nodal loops cross  $E_F$  with almost no dispersion in energy. Second, between bands  $(N - 2)$  and  $(N - 1)$  (NL1), as well as between bands  $(N + 2)$  and  $(N + 3)$  (NL5), there are nodal chains in addition to nodal loops on the  $k_x = 0$

and  $k_y = 0$  planes. In NL1 and NL5 we also found 12 and 8 Weyl points, respectively, all of which have the Chern number of  $\pm 1$ . Considering the present symmetries, the number of symmetry-inequivalent Weyl points are 3 and 2, respectively. Third, between bands  $(N - 1)$  and  $N$  (NL2), and bands  $(N + 1)$  and  $(N + 2)$  (NL4), we found more complex band degeneracies composed of extended nodal lines, nodal loops and finally essential nodal lines and surfaces. We conclude that the nodal surfaces with  $k_z = \pm\pi/c$  are protected by the composite symmetry  $\mathcal{T} \cdot \tilde{C}_{2z}$  with SOC and no inversion symmetry [37, 38].

The robustness of Weyl points can be proved by their non-zero chirality and that of nodal surfaces is guaranteed by their origin from essential degeneracy. Thus, we only need to confirm the stability of nodal lines. Their robustness is ensured by nonsymmorphic symmetries of OsOF<sub>5</sub> as described above and they can be further topologically protected by the  $\pi$  Berry phase [39]. For this purpose, we calculated the Zak phase to integrate the Berry potential along a reciprocal vector  $\mathbf{b}_1$  (parallel to  $k_x$ ) starting from the  $k$  points on the  $k_x = 0$  plane. As can be seen in Fig. 3(c), the Zak phase for the NL3 changes discontinuously from 0 to  $\pi$  across the nodal line, yielding the  $\pi$  Berry phase for any rectangular loop interlinking with it. This demonstrates the topological protection of nodal rings (NL3) crossing  $E_F$ .

The quantized  $\pi$  Berry phase is also closely related to the surface states of topological nodal-line semimetals [39, 40]. It is known that in contrast to other topological phases, the boundary states of topological nodal-line semimetals are not fully protected in that the surface states can be pushed out of the gap and merged into the bulk states [18, 41], but their connectivity with the projections of the nodal lines is protected [41], forming the so-called drumhead surface states [40, 42]. Their presence characteristic of topological nodal-line semimetals can lead to a topological polarization [43] and a possible surface superconducting order originating from a large density of states due to their weak energy dispersion [42].

Figure 4(a) shows the calculated surface-state band dispersion revealing nearly flat drumhead surface states, indicated by the arrows, which cross  $E_F$  and connect the projections of the nodal lines. To reveal more clearly the drumhead surface states, we calculated the constant-energy map of surface bands at 4 meV below  $E_F$ . The surface states are visible inside the projections of the nodal loops [Fig. 4(b)]. In general, the drumhead surface states are expected to be confined within the projection of the nodal lines onto the surface BZ, but their band dispersion and connectivity are very sensitive to the details of the surface structure [44, 45]. As seen in Fig. 4(a), two surface states are linked across the zone border and this behavior can also be seen in Fig. 4(b). Two drumhead surface states are connected through the bulk states and this connectivity is topologically protected by nontrivial  $\mathbb{Z}_2$  index [46] on the gapped TRS-invariant planes [36]

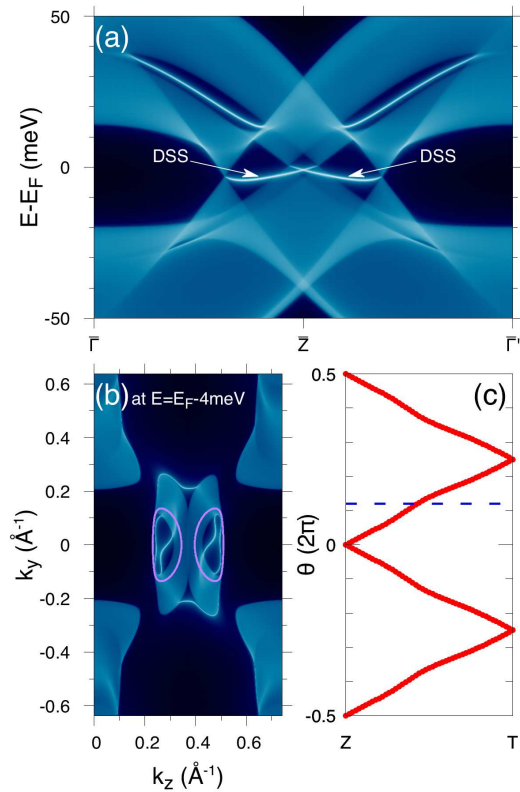


FIG. 4. (a) Momentum-resolved local density of states at the (100) surface of OsOF<sub>5</sub>. The drumhead surface states (DSSs) are indicated by white arrows. (b) Constant-energy map of (100) surface bands at  $E = E_F - 4$  meV. The projections of the nodal loops (NL3) onto the (100) surface BZ are indicated by purple lines. (c) Evolution of Wilson-loop eigenvalues  $\theta$  for the half-filled eight-band manifold on the gapped TRS-invariant plane with  $k_z = \pi/c$ . The odd number of crossing with the reference line indicates the nontrivial  $\mathbb{Z}_2$  index.

between two nodal loops, as seen in Fig. 4(c).

To conclude, we report a complex topological semimetal phase in OsOF<sub>5</sub> and investigate it in detail by performing first-principles calculations. A series of band degeneracies of different dimensionalities—Weyl points, nodal lines and nodal surfaces—are shown to coexist in a partially filled eight-band manifold. The unique feature of this material is that these topological band degeneracies are confined within a narrow energy range close to the Fermi level, a consequence of its molecular crystal structure. While being a new member of the emerging family of topological semimetals, OsOF<sub>5</sub> can also be related to the class of organic charge-transfer molecular crystals in which Mott insulating, superconducting, spin liquid and other phases [47] along with the topologically protected band degeneracies [48, 49] have been extensively investigated. Similarly, we expect novel exotic physical phenomena to be observed in OsOF<sub>5</sub>.

We thank D. Gosálbez-Martínez for helpful discussions. This work was supported by the European Re-

search Council starting grant “TopoMat” (Grant No. 306504) and the NCCR MARVEL, funded by the Swiss National Science Foundation. First-principles computations have been performed at the Swiss National Super-computing Centre under Project No. s832.

\* E-mail: hyungjun.lee@epfl.ch

† E-mail: oleg.yazyev@epfl.ch

- [1] R. P. Feynman, R. B. Leighton, and M. Sands, The Feynman Lectures on Physics, Vol. 1 (Addison-Wesley, New York, 1965).
- [2] K. Brading and E. Castellani, eds., Symmetries in Physics: Philosophical Reflections (Cambridge University Press, Cambridge, England, 2003).
- [3] M. Livio, *Nature* **490**, 472 (2012).
- [4] E. Witten, *Nat. Phys.* **14**, 116 (2018).
- [5] D. J. Gross, *Proc. Natl. Acad. Sci. U.S.A.* **93**, 14256 (1996).
- [6] E. Noether, *Nachr. kgl. Ges. Wiss. Göttingen* **235** (1918).
- [7] L. D. Landau and E. M. Lifshitz, Statistical Physics, 3rd ed., Part I. Course of Theoretical Physics, Vol. 5 (Butterworth-Heinemann, Oxford, UK, 1980).
- [8] X.-G. Wen, *Rev. Mod. Phys.* **89**, 041004 (2017).
- [9] M. Dresselhaus, G. Dresselhaus, and A. Jorio, Group Theory: Application to the Physics of Condensed Matter (Springer, New York, 2008).
- [10] L. P. Bouckaert, R. Smoluchowski, and E. Wigner, *Phys. Rev.* **50**, 58 (1936).
- [11] C. Herring, *Phys. Rev.* **52**, 365 (1937).
- [12] X. Wan, A. M. Turner, A. Vishwanath, and S. Y. Savrasov, *Phys. Rev. B* **83**, 205101 (2011).
- [13] S. M. Young, S. Zaheer, J. C. Y. Teo, C. L. Kane, E. J. Mele, and A. M. Rappe, *Phys. Rev. Lett.* **108**, 140405 (2012).
- [14] H. Nielsen and M. Ninomiya, *Phys. Lett. B* **130**, 389 (1983).
- [15] N. P. Armitage, E. J. Mele, and A. Vishwanath, *Rev. Mod. Phys.* **90**, 015001 (2018).
- [16] K. Shiozaki and M. Sato, *Phys. Rev. B* **90**, 165114 (2014).
- [17] C.-K. Chiu and A. P. Schnyder, *Phys. Rev. B* **90**, 205136 (2014).
- [18] C. Fang, H. Weng, X. Dai, and Z. Fang, *Chin. Phys. B* **25**, 117106 (2016).
- [19] S.-Y. Yang, H. Yang, E. Derunova, S. S. P. Parkin, B. Yan, and M. N. Ali, *Adv. Phys.* **X 3**, 1414631 (2018).
- [20] H. Weng, Y. Liang, Q. Xu, R. Yu, Z. Fang, X. Dai, and Y. Kawazoe, *Phys. Rev. B* **92**, 045108 (2015).
- [21] S.-M. Huang, S.-Y. Xu, I. Belopolski, C.-C. Lee, G. Chang, B. Wang, N. Alidoust, G. Bian, M. Neupane, C. Zhang, S. Jia, A. Bansil, H. Lin, and M. Z. Hasan, *Nat. Commun.* **6**, 7373 (2015).
- [22] H. Weng, C. Fang, Z. Fang, B. A. Bernevig, and X. Dai, *Phys. Rev. X* **5**, 011029 (2015).
- [23] Y. Kim, B. J. Wieder, C. L. Kane, and A. M. Rappe, *Phys. Rev. Lett.* **115**, 036806 (2015).
- [24] R. Yu, H. Weng, Z. Fang, X. Dai, and X. Hu, *Phys. Rev. Lett.* **115**, 036807 (2015).
- [25] N. Bartlett and N. K. Jha, *J. Chem. Soc. A*, 536 (1968).
- [26] N. Bartlett and J. Trotter, *J. Chem. Soc. A*, 543 (1968).
- [27] H. Shorafa and K. Seppelt, *Inorg. Chem.* **45**, 7929 (2006).
- [28] We also investigated the structure with SG *Pnma*, but the main conclusions of our work don’t change. The differences are: (1) the nodal lines are fourfold degenerate and (2) there are no Weyl points and nodal surfaces. Both of them are attributable to the presence of inversion symmetry in SG *Pnma*.
- [29] A. Bouhon and A. M. Black-Schaffer, arXiv:1710.04871 [cond-mat].
- [30] See Supplemental Material at <http://link.aps.org/supplemental/...> for the details of the computational methods.
- [31] H. Watanabe, H. C. Po, M. P. Zaletel, and A. Vishwanath, *Phys. Rev. Lett.* **117**, 096404 (2016).
- [32] R. Chen, H. C. Po, J. B. Neaton, and A. Vishwanath, *Nat. Phys.* **14**, 55 (2018).
- [33] L. Michel and J. Zak, *Phys. Rev. B* **59**, 5998 (1999).
- [34] S. M. Young and C. L. Kane, *Phys. Rev. Lett.* **115**, 126803 (2015).
- [35] B. J. Wieder and C. L. Kane, *Phys. Rev. B* **94**, 155108 (2016).
- [36] T. Bzdusek, Q. Wu, A. Rüegg, M. Sigrist, and A. A. Soluyanov, *Nature* **538**, 75 (2016).
- [37] Q.-F. Liang, J. Zhou, R. Yu, Z. Wang, and H. Weng, *Phys. Rev. B* **93**, 085427 (2016).
- [38] W. Wu, Y. Liu, S. Li, C. Zhong, Z.-M. Yu, X.-L. Sheng, Y. X. Zhao, and S. A. Yang, *Phys. Rev. B* **97**, 115125 (2018).
- [39] Y.-H. Chan, C.-K. Chiu, M. Y. Chou, and A. P. Schnyder, *Phys. Rev. B* **93**, 205132 (2016).
- [40] A. A. Burkov, M. D. Hook, and L. Balents, *Phys. Rev. B* **84**, 235126 (2011).
- [41] A. A. Burkov, *Phys. Rev. B* **97**, 165104 (2018).
- [42] N. B. Kopnin, T. T. Heikkilä, and G. E. Volovik, *Phys. Rev. B* **83**, 220503 (2011).
- [43] S. T. Ramamurthy and T. L. Hughes, *Phys. Rev. B* **95**, 075138 (2017).
- [44] G. Bian, T.-R. Chang, H. Zheng, S. Velury, S.-Y. Xu, T. Neupert, C.-K. Chiu, S.-M. Huang, D. S. Sanchez, I. Belopolski, N. Alidoust, P.-J. Chen, G. Chang, A. Bansil, H.-T. Jeng, H. Lin, and M. Z. Hasan, *Phys. Rev. B* **93**, 121113 (2016).
- [45] G. Bian, T.-R. Chang, R. Sankar, S.-Y. Xu, H. Zheng, T. Neupert, C.-K. Chiu, S.-M. Huang, G. Chang, I. Belopolski, D. S. Sanchez, M. Neupane, N. Alidoust, C. Liu, B. Wang, C.-C. Lee, H.-T. Jeng, C. Zhang, Z. Yuan, S. Jia, A. Bansil, F. Chou, H. Lin, and M. Z. Hasan, *Nat. Commun.* **7**, 10556 (2016).
- [46] C. L. Kane and E. J. Mele, *Phys. Rev. Lett.* **95**, 146802 (2005).
- [47] B. J. Powell and R. H. McKenzie, *Rep. Prog. Phys.* **74**, 056501 (2011).
- [48] A. Kobayashi, S. Katayama, Y. Suzumura, and H. Fukuyama, *J. Phys. Soc. Jpn.* **76**, 034711 (2007).
- [49] B. Commeau, R. M. Geilhufe, G. W. Fernando, and A. V. Balatsky, *Phys. Rev. B* **96**, 125135 (2017).